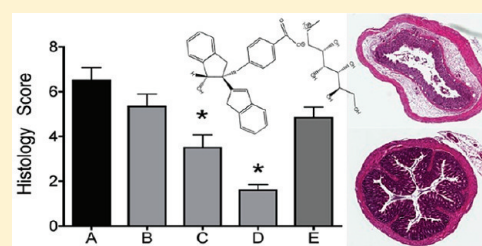


6-(Methylamino)hexane-1,2,3,4,5-pentanol 4-(((1*S*,2*S*)-1-Hydroxy-2,3-dihydro-1*H*,1'*H*-[2,2-biinden]-2-yl)methyl)benzoate (PH46A): A Novel Small Molecule With Efficacy In Murine Models Of Colitis

Neil Frankish* and Helen Sheridan*

Trinity College Dublin, Drug Discovery Group, School of Pharmacy and Pharmaceutical Sciences, College Green, Dublin 2, Ireland

ABSTRACT: The indane skeleton is found naturally and in several therapeutic molecules in medicinal chemistry. During our work on the anti-inflammatory activity of naturally occurring and synthetic indanes, we have synthesized a novel indane scaffold that has been optimized for both anti-inflammatory activity and bioavailability. We have evaluated our lead molecule, PH46A, in in vivo models of inflammatory bowel disease (IBD), an area of considerable unmet clinical need; current therapies are often unable to control the course of the disease. The compound significantly reduced histological damage and serum amyloid A (SAA) levels in IL-10^{-/-} colitis mice, was efficacious in the 5% dextran sulfate sodium (DSS) colitis model, and compared favorably with prednisolone in this model and supports its potential use to treat acute exacerbations of the disease. Further, the graded response to the compound may also lend itself to be used at a lower dose to maintain periods of remission.

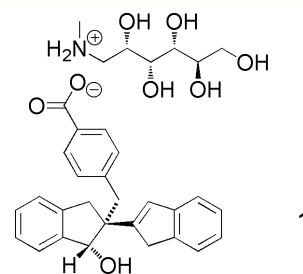


INTRODUCTION

Inflammatory bowel disease (IBD), incorporating Crohn's disease (CD) and ulcerative colitis (UC), is a chronic disease of the gastro-intestinal tract characterized by inflammation of the large and/or small intestine, with symptoms of diarrhea, abdominal pain, weight loss, and nausea. In extreme cases, it may result in malnutrition, dehydration, and anemia, which may be potentially fatal. In the U.S. alone, estimates point to 1.5 million persons being affected by the disease.¹ Environmental and genetic factors are thought to influence the course of the disease.² While patients may experience no symptoms during periods of remission, this may be interrupted with "flare-ups", acute episodes of active inflammation. There is nothing in the current pharmaceutical armamentarium to address the needs of a substantial number of sufferers for an extended period, while many patients unable to find suitable treatment will often go on to surgical intervention.³

IBD drug development has traditionally been very difficult as the disease appears to be multifactorial in etiology and many targeted therapies have failed in the clinic.^{4,5} In this study, we have assessed a lead molecule PH46A (**1**), representing a novel class of chemical compounds, in two mouse models of IBD: an acute dextran sulfate sodium (DSS) model of murine colitis⁶ and the more chronic spontaneous model of IL-10^{-/-} mice.⁷ We show that **1** has the potential to have superior efficacy to standard mainline therapy for induction of remission. Although these models do not represent all aspects of IBD in man, they bring an essential contribution to the development of much needed therapeutic solutions.

The Indane scaffold is of key importance in the natural world. It occurs in a range of biologically active natural products that have been isolated from fungi,^{8,9} bacteria,¹⁰ Pteridophytes,^{11,12} and, recently, some higher plants including the Annonaceae¹³



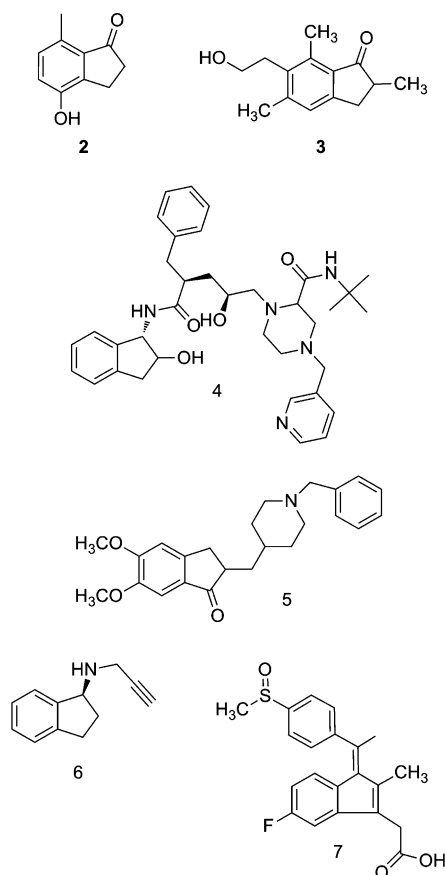
and the Dipterocarpaceae.¹⁴ The natural structures range from simple indanes and indanones with antibacterial activity, e.g., 1-indanone (**2**) isolated from the cyanobacterium *Nostoc*,¹⁰ to the pterosin family of fern and fungal metabolites, e.g., Pterosin B (**3**), which shows cytotoxicity toward the human leukemia HL-60 cell line.¹¹

The therapeutic potential of indane and indanone derived molecules becomes more evident in the area of medicinal chemistry where this scaffold is incorporated into an array of chemical structures that demonstrate significant therapeutic properties, e.g., the protease inhibitor Indinavir (**4**), in clinical use^{15,16} for the treatment of HIV-1, the indanone, Donepezil (**5**), a potent acetylcholinesterase inhibitor, which is prescribed for the treatment of Alzheimer's disease,¹⁷ the propargyl amine Rasigiline, an irreversible inhibitor of monoamine oxidase used in Parkinson's disease (**6**),¹⁸ and the indanone Sulindac (**7**), a nonsteroidal anti-inflammatory that has recently demonstrated antiproliferative and apoptotic effects.^{19,20}

The development of **1** originated in an investigation into the traditional use of indanes, derived from Pteridophytes of the

Received: March 26, 2012

Published: June 4, 2012



Onychium family, in Taiwanese traditional medicine.^{21,22} In these early studies, we established the smooth muscle relaxant and mast cell stabilization effects of nature identical and synthetic monomeric analogues.^{23–26} We subsequently synthesized and investigated a novel series of indane dimers which were shown to inhibit the release of histamine from rat peritoneal mast cells. The impetus behind the research was to identify a novel molecule which retained significant smooth muscle relaxant activity and which possessed potent mast cell stabilizing activity, a molecule which combined the effects of disodium cromoglycate with a bronchodilator and which might find utility in the treatment of asthma.^{27–29} However, while it appeared that the two activities were mutually exclusive, we successfully identified a novel indane scaffold with potential therapeutic value for the treatment of inflammatory disease.²⁸

More polar analogues of the active compounds previously described²⁸ were assessed in an inflammatory disease model, the 5% DSS model of murine colitis. Of these, **1** was chosen as the lead candidate on the basis of its efficacy. The scaffold of **1** incorporates the indane skeleton of the original molecules and is the *N*-glucamine salt of a single enantiomer of this novel drug.

The efficacy of **1** (3–30 mg/kg) was assessed in the 5% DSS murine model of colitis, characterized by weight loss, shortening of the colon, intestinal bleeding, and histological damage as well as on the IL-10^{-/-} murine model of colitis, a spontaneously developing chronic colitis characterized by weight loss, raised levels of serum amyloid A, and damage to the intestinal epithelial layer without chemically induced tissue damage.

RESULTS

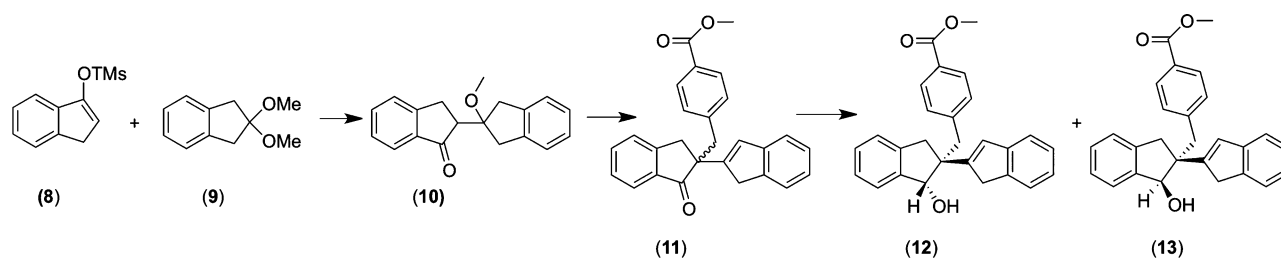
Chemistry. Compound **1** is synthesized via a key intermediate **10** formed by the coupling of the silyl trimethyl ether of 1-indanone (**8**) and the dimethyl ketal of 2-indanone (**9**) with a catalytic amount of trimethylsilyltriflate over 3 Å molecular sieves.²⁸ Intermediate **10** was then alkylated with methyl (4-bromomethyl) benzoate to yield the racemic keto ester **11**, as shown in Scheme 1.

This mixture of enantiomers was reduced with NaBH₄ to yield the diastereoisomeric esters **12** and **13**, which were separated by flash column chromatography using a TBME and EtOAc gradient. The esters were hydrolyzed quantitatively to their corresponding acids (**14** and **15**) by refluxing with 10% NaOH in MeOH. Separation of **14** and **15** into their constituent enantiomers **16**, **17** and **18**, **19**, respectively (Scheme 2) was achieved by chiral HPLC. The absolute stereochemistry of the **16** was established by single crystal X-ray analysis of its *S*-(-)- α -methylbenzylamine salt. Further, the absolute stereochemistry of **18** and **19** was established by conversion of the alcohols (**16**–**19**) to their ketones and by correlation of their optical rotations.³⁰ The acids **16** and **19** were converted into their *N*-methyl-(*D*)-glucamine salts **1** and **20** by stirring the acids in MeOH with *N*-methyl-*D*-glucamine.

PHARMACOLOGICAL EVALUATION

Effect of Enantiomers in DSS Colitis. Specific Pathogen-Free female Balb/*c* mice, 6–8 weeks of age, given 5% DSS in drinking water, were administered vehicle or **16**–**19** at 30 mg/kg po as a suspension in carboxymethyl cellulose (0.5%)/2% Tween 80 daily for 7 days. Mice administered vehicle developed progressive weight loss (Figure 1c) and increased disease activity index (DAI) values following DSS treatment (Figure 1a,b). There were no overt reactions following 7 days of daily oral (po 30 mg/kg) treatment with the compounds **16**–**19**. The DAI measures the extent of the disease in this model. **18** was without activity on this variable, there not being any significant ($P > 0.05$) difference in DAI at any time point (Figure 1a). At day 7, both **16** and **19** significantly ($P < 0.01$) reduced DAI by a considerable margin, from 9.0 ± 0.53 for vehicle controls to 2.5 ± 0.71 for **16** and 3.2 ± 0.73 for **19**, there being no significant difference between the two (Figure 1b). In comparison, **17** reduced DAI to only 5.3 ± 0.6 . This was significantly ($P > 0.05$) less potent than either **16** or **19**. Further, while the DAI in **17**-treated mice was

Scheme 1. Synthesis of Keto-ester **11** and Diastereoisomers **12** and **13** from Key Intermediate **10**



Scheme 2. Separation of Enantiomers of 12 and 13

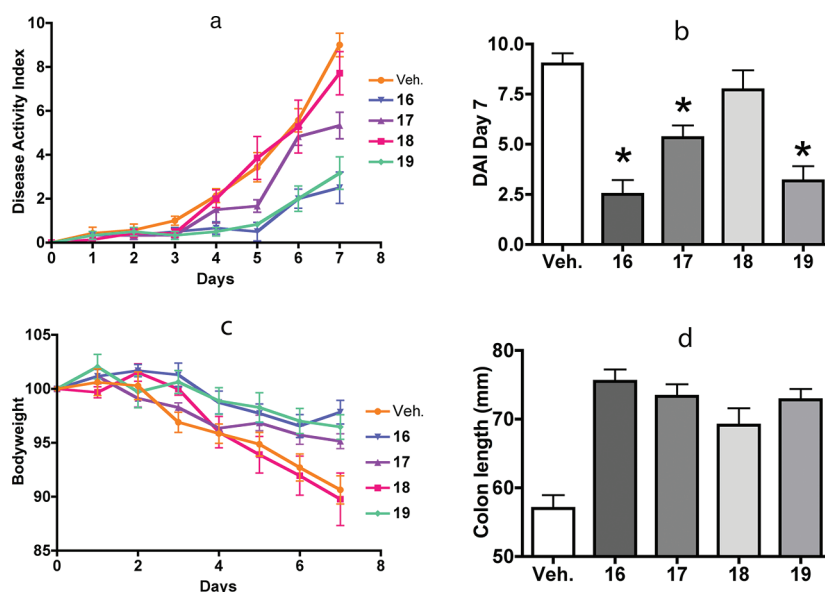
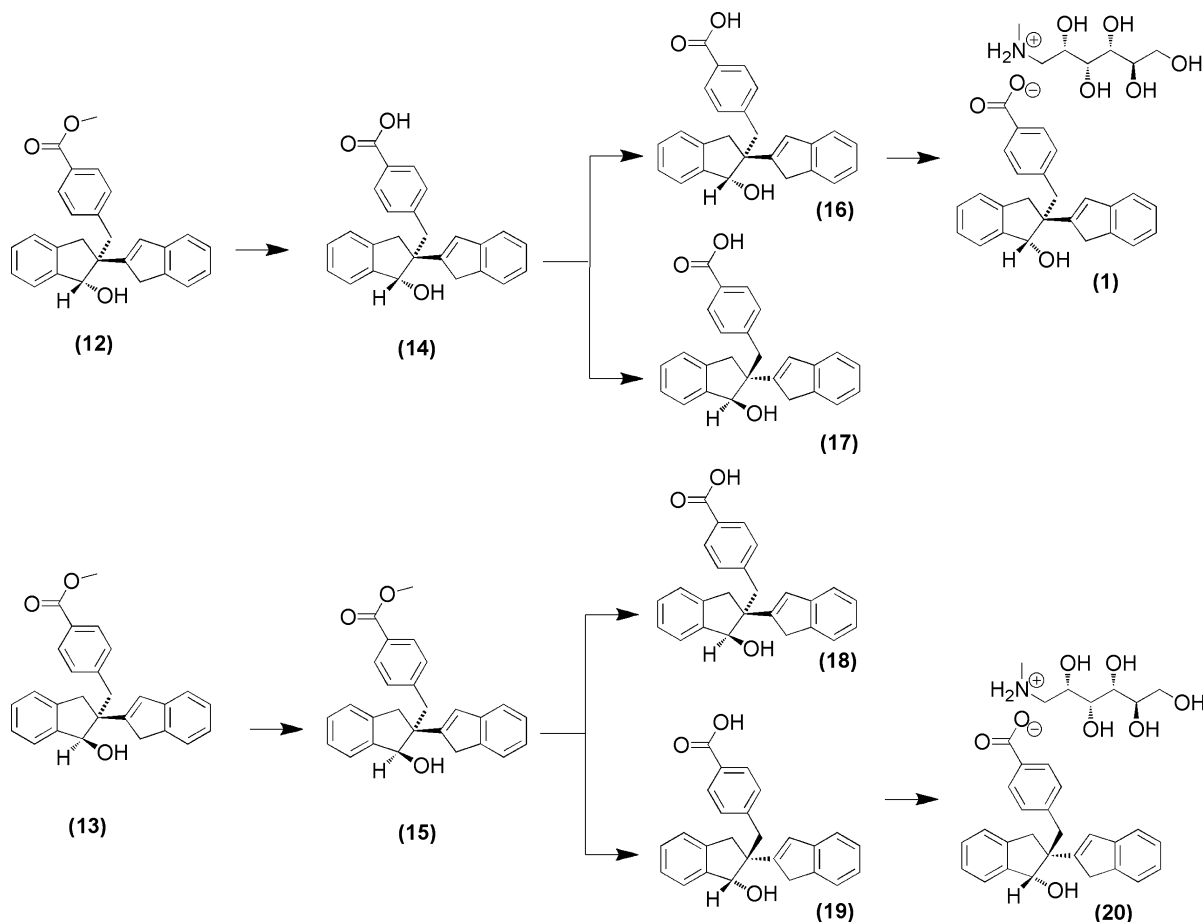


Figure 1. Effect of vehicle (Veh.) and 16–19 (30 mg/kg) on disease activity index (DAI) (a), DAI on day 7 (b), bodyweight (c), and colon length (d). Values are expressed as a mean \pm SEM, $n = 6$. Asterisks indicate statistical significance at $P < 0.01$.

statistically ($P < 0.01$) less than vehicle controls at day 7, at day 6 there was no statistical ($P > 0.05$) difference between 17 and vehicle (Figure 1a). In conclusion, of the four enantiomers, 16–19, both 16 and 19 are highly active in this model at 30 mg/kg. 17 has minimal activity which is significantly ($P < 0.01$) less than 16

and 19, and 18 is almost devoid of activity in this DSS murine colitis model. On colon length, all enantiomers increased colon length compared to vehicle control in order of potency 16 > 19 > 17 > 18 (Figure 1d).

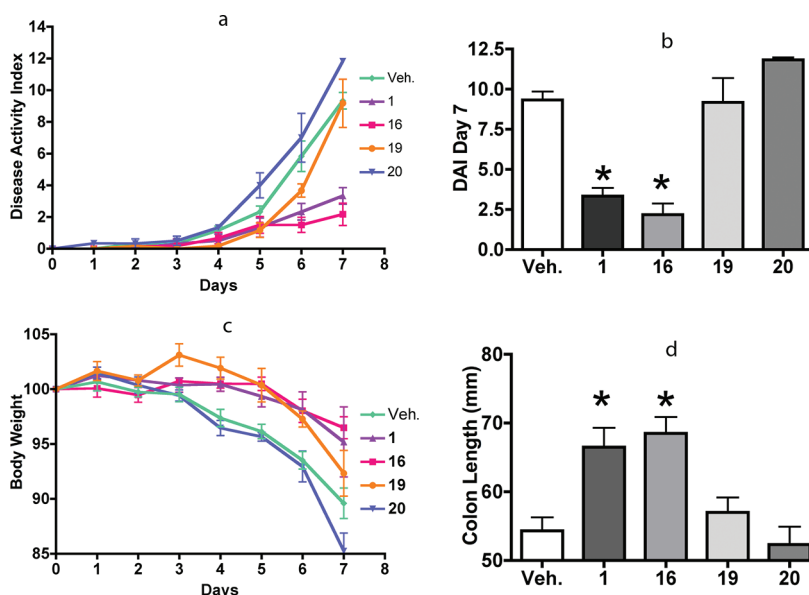


Figure 2. Effect of vehicle (Veh) and 16, 19, 1, and 20 (10 mg/kg) on disease activity index (DAI) (a), DAI on day 7 (b), body weight (c), and colon length (d). Values are expressed as a mean \pm SEM, $n = 6$. Asterisks indicate statistical significance at $P < 0.01$.

Effect of the Enantiomers 16 and 19 and Their *N*-Glucamine Salts (1, 20) at 10 mg/kg in 5% DSS Colitis.

Given that both 16 and 19 show considerable activity in the 5% DSS model at 30 mg/kg, we then re-examined their activity, together with their *N*-glucamine salts (1, 20) at the lower dose of 10 mg/kg, given daily for 7 days as a suspension or solution in carboxymethyl cellulose (0.5%)/2% Tween 80. No adjustment was made in the dosages of the salts to compensate for their increased molecular weight. Mice administered vehicle developed progressive weight loss (Figure 2c), and this was significantly ameliorated by both 16 and 1 but not by 19 and 20 at 10 mg/kg. Both 19 and 20 at 10 mg/kg had no significant ($P > 0.01$) effect on DAI in the 5%-DSS murine colitis model when compared to vehicle control (see Figure 2a,b). In contrast, at day 7, both 16 and 1 at 10 mg/kg significantly ($P < 0.01$) and potently reduced DAI from 9.3 ± 0.51 (vehicle) to 2.1 ± 0.7 and 3.3 ± 0.52 , respectively (Figure 2b). Both 16 and 1 significantly increased colon length compared to vehicle control, whereas 19 and 20 had no significant effect (Figure 2d).

In conclusion, 16, together with its *N*-glucamine salt 1, is the most potent of the four enantiomers by a considerable margin and the only enantiomer to retain activity at this dose level. As a consequence of the limited amount of material, much of the comparison solubility and PK studies were performed on compounds 19 and 20. Such studies showed that the bioavailability of the acid, 19, was only 61%, whereas that of the salt, 20, was 100%. Pharmacokinetic data on 1 has shown that it is 100% bioavailable and $>6000 \mu\text{g mL}^{-1}$ aqueously soluble.³¹ Compound 1 was therefore chosen as the preferred compound.

Graded Response to 1 in Acute DSS Colitis and a Comparison with Prednisolone.

The values of a number of disease indicators in mice treated with DSS were compared with those in mice treated with the standard steroid therapy, prednisolone (5 mg/kg), typically used for induction of remission in patients suffering from active disease. BALB/c mice, seven per group, in which an acute colitis had been induced by administering 5% DSS in the drinking water for 7 days, were assessed daily over this period. Body weight declined progressively over the 7 days, by 18.55% at day 7, but this

weight loss was reduced when DSS-mice were administered 1 (orally, per os (po)) daily, at all dose levels; at 30 mg/kg, 1 reduced weight loss to only 6.2% of non-DSS control mice. With 12.6% weight loss, prednisolone was only as effective as 10 mg/kg 1 (12.8%) (Figure 3a). In addition, the DAI began to become

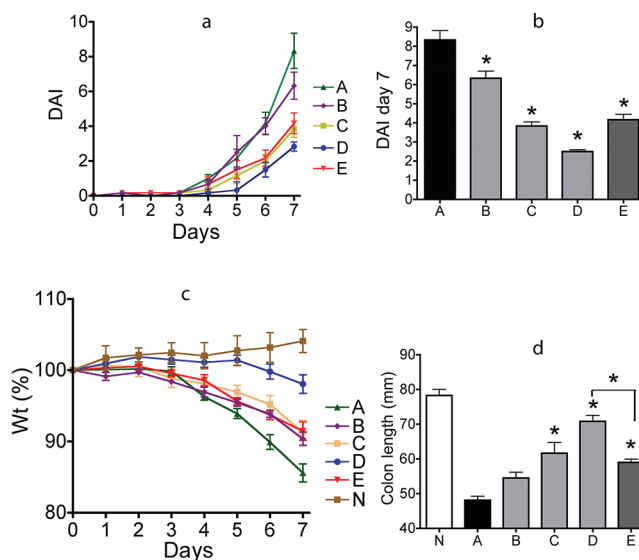


Figure 3. Effect of vehicle (A), 1 (3, 10, 30 mg/kg) (B, C, D), prednisolone (5 mg/kg) (E), and water only (non-DSS; N) on disease activity index (DAI) (a), DAI on day 7 (b), body weight (c), and colon length (d). Values are expressed as a mean \pm SEM, $n = 6-7$. Asterisks indicate statistical significance at $P < 0.01$.

elevated at day 3 and by day 4, and there was already apparent a difference in treated and nontreated groups (Figure 3a). At day 7, DAI was significantly and dose-dependently reduced by 1 to 24%, 54%, and 80% of the vehicle group for the 3, 10, and 30 mg/kg doses, respectively, while prednisolone (5 mg/kg) reduced DAI by 50% (Figure 3b). Another disease indicator measured was colon length because treatment with DSS typically results in

a shortening of the colon. By day 7, **1** reduced this shortening in a dose-dependent manner, with 30 mg/kg **1** significantly ($P < 0.01$) more effective than prednisolone at 76% and 39% inhibition, respectively (Figure 3d). Furthermore, colonic MPO activity, representing the level of inflammatory neutrophil cell infiltration into the gut wall, was increased by almost 8-fold by the DSS treatment. By day 7, both **1** at 30 mg/kg and prednisolone significantly reduced MPO by 63% and 54%, respectively (Figure 4a). In addition, DSS-treatment resulted in

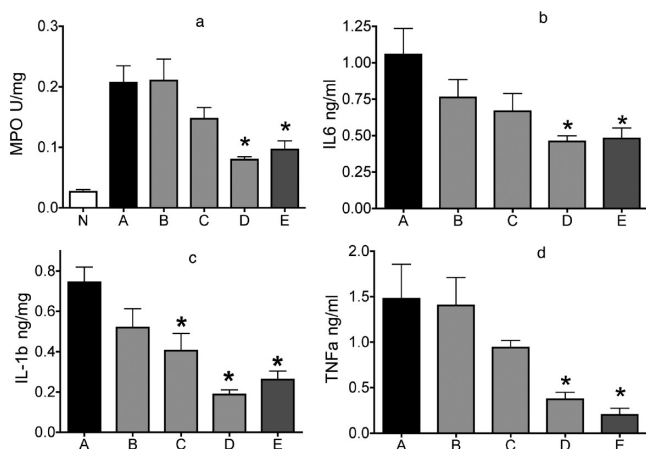


Figure 4. Effect of vehicle (A), **1** (3, 10, 30 mg/kg) (B, C, D), prednisolone (5 mg/kg) (E), and water only (non-DSS; N) on colon myeloperoxidase activity (MPO) (a), colon IL-6 levels (b), colon IL-1 β levels (c), and TNF α (d). Values are expressed as a mean \pm SEM, $n = 6-7$. Asterisks indicate statistical significance at $P < 0.01$.

raised levels of the colonic pro-inflammatory cytokines IL1 β , IL6, and TNF α , to 0.744 ± 0.076 ng/mg, 1.057 ± 0.1784 ng/mg, and 1.478 ± 0.378 ng/mg, respectively. In each case, **1** caused a significant ($P < 0.01$) and dose-dependent reduction in these cytokine levels. Prednisolone also reduced ($p < 0.01$) raised cytokine levels; for each cytokine there was no significant difference between the effect of prednisolone 5 mg/kg and **1** at the higher dose at day 7 (Figure 4). The colons were scored for histological damage. Treatment with **1** caused a marked and dose-dependent decrease in such scores, with **1** (30 mg/kg) reducing histological damage scores from 6.5 ± 0.56 for vehicle control to 1.6 ± 0.24 , i.e., by more than 75%. In comparison, the effect of prednisolone on reducing histological damage scores, at 26% (4.8 ± 0.48) (Figure 5), did not achieve statistical significance ($P > 0.05$).

Treatment of IL-10 Deficient Mice with 1. IL-10 $^{-/-}$ BALB/c strain mice were treated from 6 to 8 weeks of age, when colon inflammation is mild,⁷ with **1** (300 mg/kg/week) or vehicle on a Mon/Wed/Fri dosing schedule over a period of 9 weeks. There was no significant differences in weight loss or overt colitis—rectal bleeding or prolapse requiring humane killing of mice between vehicle-treated (3/12 mice killed) and **1**-treated (1/12 mice killed) IL-10 $^{-/-}$ mice. After 9 weeks, serum was recovered from mice and SAA analyzed as a marker for the severity of colitis. In IL-10 $^{-/-}$ mice treated with **1**, there were significantly ($P < 0.05$) decreased SAA levels relative to vehicle-treated mice (468.9 ± 38.37 to 342.7 ± 43.01 μ g/mL) (Figure 6a). Histology sections of colons from IL-10 $^{-/-}$ mice treated with vehicle and **1** (Figure 6c,d) were scored for histological damage. The extent of colon pathology was significantly reduced ($P < 0.05$) in IL-10 $^{-/-}$ mice receiving **1** (score: 4.18 ± 0.48),

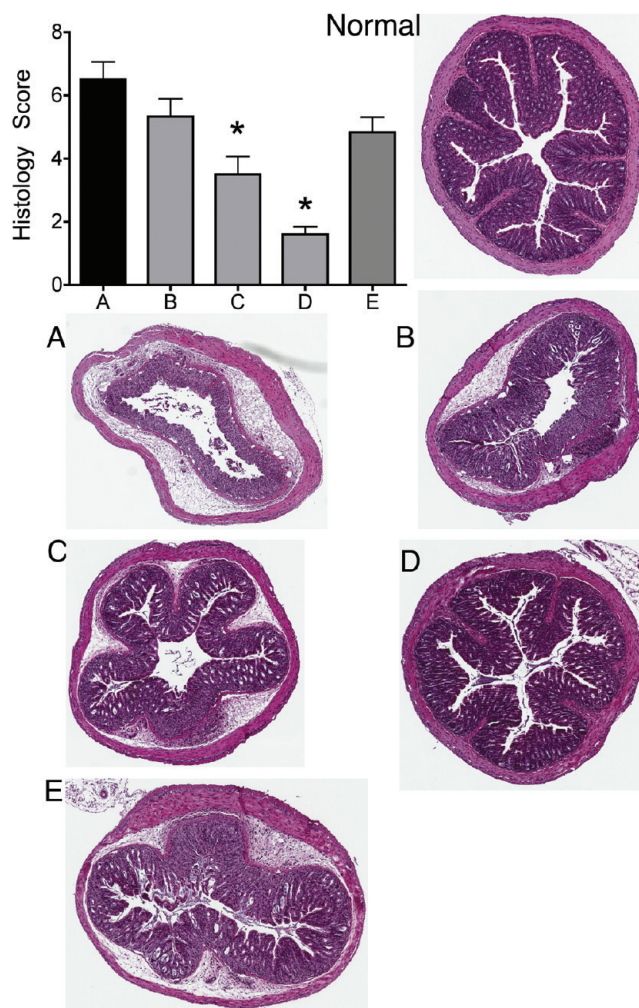


Figure 5. Scoring of colons from DSS-treated mice administered (A), **1** (3, 10, 30 mg/kg) (B, C, D), and prednisolone (5 mg/kg) (E). Representative H&E stained sections of distal colon of untreated (normal) mice and animals treated with DSS and compounds as indicated for 7 days. Colon of normal, non-DSS-treated, mouse (normal). Colon of 5% DSS-treated mice injected with saline (A) with 3, 10, and 30 mg/kg **1** (B, C, D), or 5 mg/kg prednisolone (E).

relative to mice treated with vehicle (score: 6.22 ± 0.72) (Figure 6b). These data indicate that chronic treatment of IL-10 $^{-/-}$ with **1** significantly ameliorates clinical indicators of colitis in this model.

DISCUSSION

In this study, we evaluated the efficacy of the novel, anti-inflammatory indane compound, **1**, in two distinct murine colitis models. Oral treatment of mice with **1** attenuated the severity of colitis in an acute DSS model of colitis. Furthermore, chronic administration of **1** to IL-10 $^{-/-}$ mice ameliorated the spontaneous development of colonic inflammation. As **1** has efficacy in two distinct acute and chronic mouse models of IBD, which are engendered by diverse mechanisms, the drug's therapeutic effect is independent of the model. These data indicate that **1** has potential for the development of a drug therapy in the treatment of IBD.

Traditionally, IBD patients were maintained on remission by use of a 5-aminosalicylate. While its use in UC provides considerable benefit, both in inducing remission in mild to

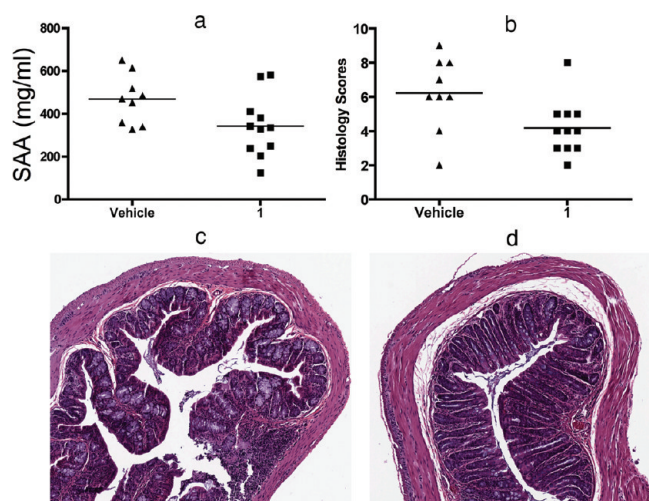


Figure 6. Effect of **1** (300 mg/kg week) in IL-10^{-/-} mice. (a) Histology scores of colon damage. (b) Serum amyloid A (SAA) levels. Representative H&E stained sections of mouse colon of untreated IL-10^{-/-} mice. Values are expressed as mean \pm SEM, $n = 9$ and 11 for vehicle and **1** groups, respectively (c), showing breakdown of the mucosal epithelium and crypt erosion with cell infiltration of mice treated with **1** (d), showing substantially less epithelial damage and limited cell infiltration.

moderate disease and in preventing relapse,³² its usefulness to maintain remission in CD is questionable and no longer recommended, leaving patients with mild CD few options for maintenance therapy.¹ In contrast, the mainstay of treatment of active disease is a corticosteroid, used for limited periods to return both UC and CD patients to remission. However, systemic corticosteroids such as prednisolone are associated with adverse effects, while nonsystemic budesonide, which has fewer side-effects, does not maintain remission.³³ Compound **1**, with a potentially more favorable toxicological profile than corticosteroids, could thus provide an alternative, at the least in cases of steroid resistance, or in a steroid-sparing regimen. Indeed, our toxicological and toxicokinetic studies have shown a maximum tolerated dose (MTD) of >2000 mg/kg in rats and >500 mg/kg in dogs.³⁴ In addition, **1** could also help avoid serious adverse effects³ of alternative treatments such as the immunosuppressive drugs azathioprine and mercaptopurine as well as methotrexate and cyclosporine. Further, effective alternatives such as the anti-TNF α antibodies, infliximab, and adalimumab have, however, not proven efficacious in all patients. There could therefore be an opportunity to treat anti-TNF α nonresponders with **1** without a generalized immunosuppression and subsequent development of opportunistic infections.

In the acute DSS model of colitis, **1** can substantially reduce disease severity, as ascertained by multiple parameters. Furthermore, in the chronic spontaneous IL-10^{-/-} mouse model, **1** ameliorated development of colitis. In these two models of colitis, disease is evoked by distinct processes that range from maintenance of epithelial barrier and its integrity to aberrant regulation of innate and adaptive immune homeostasis in the gastro-intestinal tract. This infers that **1** suppresses colon inflammation via a protective process, as yet unknown, that is common to both models. Elucidation of the mechanism of action of **1** in reducing inflammation in colitis will lead to new insights into the development of IBD and opportunities to develop further new therapeutic strategies.

CONCLUSIONS

Compound **1** has significant activity in the IL-10^{-/-} model of IBD and is highly efficacious in the acute DSS model. This efficacy compares favorably with the potent steroid, prednisolone, and supports its potential use to treat acute exacerbations of the disease. Further, the graded response to **1** may also lend itself to be used at a lower dose to maintain periods of remission. This small molecule represents a new class of compounds for the treatment of IBD.

EXPERIMENTAL SECTION

Chemistry. Melting points were determined on a Me-Opta hot stage and are uncorrected. Nuclear magnetic resonance spectra (NMR) were recorded using a Bruker Avance 400 instrument. ¹H NMR spectra were recorded at 400.13 MHz, and ¹³C NMR spectra were recorded at 75.47 MHz. Chemical shifts are given in parts per million (ppm) and were referenced to solvent signals. COSY, HSQC, and HBMIC were performed using Bruker microprograms. Spectra were analyzed using MestRec Magnetic Resonance Companion version 4.4.1.0. High resolution mass spectra were determined on a Micromass LCT instrument operating in ES⁺ mode. HPLC was performed on a reverse phase 250 mm \times 4.6 mm Hypersil BDS C18, 5 μ , column using a Waters 600 chromatograph equipped with an auto sampler, column oven, and dual wavelength detector. The flow rate was 1 mL/min (for ketone and esters) and 0.6 mL/min (for acids and salts) with isocratic elution with a mobile phase consisting of 70:30 CH₃CN/0.1% aq acetic acid. Detection: 210 nm. The column temperature was room temperature. TLC was performed on commercially precoated plates (Merck, Kieselgel 60F₂₅₄). Flash column chromatography was carried out on Merck Kieselgel 60 (200–400 mesh) (E. Merck, Art 9385, Darmstadt). Visualization was by examination under visible light UV (254 nm) and UV (365 nm) or by spraying with anisaldehyde/concd sulphuric acid reagent followed by heating for 5–10 min at 110 $^{\circ}$ C. Test compounds **1** and **16–20** were >98% pure by HPLC.

Preparation of (1*H*-inden-3-yl)trimethylsilane (**8**), 2,2-dimethoxy-2,3-dihydro-1*H*-indene (**9**), and 2,3-dihydro-2-(2,3-dihydro-2-methoxy-1*H*-inden-2-yl)inden-1-one (**10**) are outlined in Sheridan et al 2009.²⁸

Methyl 4-((2,3-Dihydro-2-(1*H*-inden-2-yl)-1-oxo-1*H*-inden-2-yl)methyl)benzoate (11**).** To a stirred solution of **10** (1.00 g, 4 mmol) in *tert*-butanol (5 mL) and diethyl ether (30 mL) was added methyl (4-bromomethyl)benzoate (1.41 g, 6 mmol). To this was added a solution of potassium *tert*-butoxide in *tert*-butanol (30 mL), slowly, dropwise. With each drop, the mixture turned a yellow color and then reverted to its original gray color. The mixture was stirred for further 3 h until the TLC (hexane/EtOAc, 4:1) showed no more starting material. The reaction was quenched by the addition of satd NH₄Cl. The layers were separated and the aqueous layer extracted with diethyl ether (2 \times 120 mL). The combined organic extracts were washed with water and brine, dried over MgSO₄, and evaporated in vacuo. The solid product precipitated from the crude on removal of most of the solvent. This was filtered off and washed with cold diethyl ether to give compound **11** (0.98 g, 62%) as a cream solid; mp 143–147 $^{\circ}$ C. ¹H NMR (400 MHz, CDCl₃) δ _H (ppm) 7.87 (d, $J = 7.52$ Hz, 2H), 7.74 (d, $J = 7.68$ Hz, 1H), 7.57 (t, $J = 7.48$ Hz, 1H), 7.40 (d, $J = 7.56$ Hz, 2H), 7.36 (t, $J = 7.48$ Hz, 1H), 7.30–7.14 (m, 5H), 6.74 (s, 1H), 3.88 (s, 3H), 3.61–3.31 (m, 6H). ¹³C NMR (100 MHz, CDCl₃) δ _C (ppm) 205.2, 166.5, 151.8, 148.3, 143.7, 142.7, 142.5, 134.7, 2 \times 129.6, 2 \times 129.0, 128.2, 128.0, 127.3, 126.0, 125.7, 124.3, 124.2, 123.1, 120.3, 56.7, 51.6, 41.8, 38.4, 37.2. HRMS (ESI) m/z calculated for C₂₇H₂₂O₃ (M + Na)⁺, 471.1474; found, 471.1461.

Methyl 4-((2,3-Dihydro-1-hydroxy-2-(1*H*-inden-2-yl)-1*H*-inden-2-yl)methyl)benzoate (12**) and (**13**).** To a stirred solution of **11** (2.00 g, 5.07 mmol) in MeOH (20 mL) and tetrahydrofuran (20 mL) was added NaBH₄ (0.29 g, 7.61 mmol), slowly (10 min), portionwise at 0 $^{\circ}$ C. The temperature of the reaction was maintained between 0 and 5 $^{\circ}$ C throughout the reaction. The mixture was stirred for further 3 h until the TLC (hexane/EtOAc/DCM, 5:1:1) showed no more starting material.

On completion, the reaction was quenched by the addition of water (30 mL) and MeOH was removed from the reaction mixture under vacuum. The resulting residue was extracted between water (30 mL) and diethyl ether (3 × 25 mL). The combined organic extracts were washed with water and brine, dried over MgSO₄, and evaporated in vacuo. The residue was purified by flash column chromatography on silica gel (eluent: hexane/EtOAc/DCM, 5:1:1). All homogeneous fractions were collected and the solvent was evaporated to afford compounds **12** (1.07 g, 54%) and **13** (0.97 g, 49%) as white amorphous solids.

Compound (12). Melting point 141–143 °C. ¹H NMR (400 MHz, CDCl₃) δ_H (ppm) 6.99 (d, *J* = 7.72 Hz, 2H), 7.46 (d, *J* = 7.04 Hz, 2H), 7.20–7.31 (m, 6H), 6.97 (d, *J* = 7.80 Hz, 2H), 6.50 (s, 1H), 5.29 (d, *J* = 24.16 Hz, 1H), 3.91 (s, 3H), 3.60 (d, *J* = 22.68 Hz, 1H), 3.48 (d, *J* = 22.88 Hz, 1H), 3.28 (d, *J* = 13.24 Hz, 1H), 3.06 (d, *J* = 15.64 Hz, 1H), 3.51 (d, *J* = 16.00 Hz, 1H), 2.86 (d, *J* = 13.28 Hz, 1H). ¹³C NMR (100 MHz, CDCl₃) δ_C (ppm) 166.9, 152.3, 144.1, 143.9, 143.4, 142.4, 140.0, 2 × 129.8, 2 × 128.6, 128.1, 128.0, 127.5, 126.6, 126.0, 124.4, 123.9, 123.6, 123.2, 120.2, 82.4, 55.5, 51.6, 39.6, 38.2, 38.0. HRMS (ESI) *m/z* calculated for C₂₇H₂₄O₃ (M + Na)⁺, 419.1606; found, 419.1618.

Compound (13). Melting point 161–163 °C. ¹H NMR (400 MHz, CDCl₃) δ_H (ppm) 7.87 (d, *J* = 8.12 Hz, 2H), 7.45 (d, *J* = 7.04 Hz, 1H), 7.42 (d, *J* = 7.40 Hz, 1H), 7.35–7.26 (m, 5H), 7.19 (d, *J* = 7.40 Hz, 1H), 7.02 (d, *J* = 8.16 Hz, 2H), 6.69 (s, 1H), 5.07 (d, *J* = 7.92 Hz, 1H), 3.90 (s, 3H), 3.55 (d, *J* = 22.68 Hz, 1H), 3.37 (d, *J* = 22.76 Hz, 1H), 3.27 (d, *J* = 15.88 Hz, 1H), 3.26 (d, *J* = 13.48 Hz, 1H), 2.95 (d, *J* = 15.76 Hz, 1H), 2.93 (d, *J* = 13.60 Hz, 1H). ¹³C NMR (100 MHz, CDCl₃) δ_C (ppm) 166.6, 149.9, 143.8, 143.1, 143.0, 142.7, 141.0, 130.3, 2 × 129.7, 2 × 128.8, 128.4, 127.8, 126.7, 126.0, 124.6, 124.5, 124.1, 123.1, 120.3, 81.6, 55.9, 51.6, 43.0, 39.9, 37.9. HRMS (ESI) *m/z* calculated for C₂₇H₂₄O₃ (M + Na)⁺, 419.1605; found, 417.1618.

Hydrolysis of Methyl Ester (12) or (13). The methyl ester was placed in a round-bottomed flask and 10% aq NaOH (1 mL) was added to it, followed by sufficient MeOH to form a solution (6 mL). The resulting mixture was stirred under reflux conditions, and the reaction was monitored by TLC (hexane/EtOAc, 4:1). After 24 h, no further ester was seen. The mixture was cooled, and satd aq NH₄Cl (10 mL) was added (solution at pH = 12). The mixture was acidified with 2 M aq HCl until pH = 2. The product was extracted from the cloudy solution into EtOAc (3 × 20 mL). The combined extracts were dried over MgSO₄ and evaporated in vacuo to give target compound (quantitative). The crude material could be isolated in very pure form by slurry in a solvent mixture of hexane/MTBE (v/v, 80:20). The yield from this step was generally >95% of **14** or **15** as cream solids.

Separation of (14) to Yield (16) and (17). Enantiomers were separated by preparative Chiral HPLC: column 250 mm × 76 mm CHIRALPAK AZ 20 μm, detection UV 203 nm, flow rate 250 mL/min. Mobile phase 100:0:1, methanol/acetic acid. Rt (**16**) 6.65 min; Rt (**17**) 8.48 min.

4-(((1S,2S)-2,3-Dihydro-1-hydroxy-2-(1H-inden-2-yl)-1H-inden-2-yl)methyl)benzoic Acid (16). Melting point 184–185 °C. Optical rotation [α]_D²⁰ = −162.5° (MeOH, 40 mg/10 mL, 20 °C). ¹H NMR (400 MHz, CDCl₃) δ_H (ppm) 7.90 (d, *J* = 8.04 Hz, 2H), 7.44 (d, *J* = 7.08 Hz, 2H), 7.25–7.34 (m, 5H), 7.18 (dt, *J* = 7.03, 1.75 Hz, 1H), 7.00 (d, *J* = 8.08 Hz, 2H), 6.49 (s, 1H), 5.27 (s, 1H), 3.58 (d, *J* = 22.64 Hz, 1H), 3.46 (d, *J* = 22.64 Hz, 1H), 3.29 (d, *J* = 13.32 Hz, 1H), 3.07 (d, *J* = 15.64 Hz, 1H), 3.02 (d, *J* = 15.60 Hz, 1H), 2.87 (d, *J* = 13.52 Hz, 1H). ¹³C NMR (100 MHz, CDCl₃) δ_C (ppm) 171.0, 152.0, 144.7, 144.0, 143.2, 142.3, 140.0, 2 × 129.9, 2 × 129.3, 128.2, 128.1, 126.6, 126.5, 126.0, 124.5, 123.9, 123.5, 123.1, 120.2, 82.4, 55.5, 39.5, 38.2, 38.1. HRMS (ESI) *m/z* calculated for C₂₆H₂₂O₃ (M − H)⁺, 381.1485; found, 381.1501.

4-(((1R,2R)-2,3-Dihydro-1-hydroxy-2-(1H-inden-2-yl)-1H-inden-2-yl)methyl)benzoic Acid (17). Melting point 195–196 °C. Optical rotation [α]_D²⁰ = +127.5° (MeOH, 40 mg/10 mL, 20 °C). ¹H NMR (400 MHz, CDCl₃) δ_H (ppm) 7.90 (d, *J* = 7.32 Hz, 2H), 7.44 (d, *J* = 6.96 Hz, 2H), 7.25–7.31 (m, 5H), 7.18 (t, *J* = 6.90 Hz, 1H), 7.00 (d, *J* = 7.56 Hz, 2H), 6.49 (s, 1H), 5.27 (s, 1H), 3.58 (d, *J* = 22.60 Hz, 1H), 3.46 (d, *J* = 22.52 Hz, 1H), 3.29 (d, *J* = 13.28 Hz, 1H), 3.07 (d, *J* = 16.00 Hz, 1H), 3.02 (d, *J* = 15.80 Hz, 1H), 2.87 (d, *J* = 13.32 Hz, 1H). ¹³C NMR (100 MHz, CDCl₃) δ_C (ppm) 171.2, 152.0, 144.7, 144.0, 143.2, 142.3, 140.0,

2 × 129.9, 2 × 129.3, 128.2, 128.1, 126.6, 126.5, 126.0, 124.5, 123.9, 123.5, 123.1, 120.2, 82.4, 55.5, 39.5, 38.2, 38.1. HRMS (ESI) *m/z* calculated for C₂₆H₂₂O₃ (M − H)⁺, 381.1485; found, 381.1494.

Separation of (15) to Yield (18) and (19). Enantiomers were separated by preparative Chiral HPLC: column 250 mm × 76 mm CHIRALCEL OJ 20 μm, detection UV 203 nm, flow rate 500 mL/min. Mobile phase methanol, Rt (**18**) 13.6 min; Rt (**19**) 21.4 min.

4-(((1R,2S)-2,3-Dihydro-1-hydroxy-2-(1H-inden-2-yl)-1H-inden-2-yl)methyl)benzoic Acid (18). Melting point 136–140 °C. Optical rotation [α]_D²⁰ = −39.3° (MeOH, 0.66%, 20 °C). ¹H NMR (400 MHz, CDCl₃) δ_H (ppm) 7.93 (d, *J* = 8.08 Hz, 2H), 7.26–7.47 (m, 7H), 7.19 (t, *J* = 7.34 Hz, 1H), 7.05 (d, *J* = 8.08 Hz, 2H), 6.70 (s, 1H), 5.08 (s, 1H), 2.90–3.59 (m, 6H). ¹³C NMR (100 MHz, CDCl₃) δ_C (ppm) 171.2, 149.8, 144.1, 143.8, 143.0, 142.7, 141.0, 130.4, 2 × 129.8, 2 × 129.4, 128.5, 126.9, 126.7, 126.0, 124.7, 124.5, 124.1, 123.2, 120.3, 81.6, 55.9, 43.1, 39.9, 37.9. HRMS (ESI) *m/z* calculated for C₂₆H₂₂O₃ (M − H)⁺, 381.1485; found, 381.1494.

4-(((1S,2R)-2,3-Dihydro-1-hydroxy-2-(1H-inden-2-yl)-1H-inden-2-yl)methyl)benzoic Acid (19). Melting point 195–196 °C. Optical rotation [α]_D²⁰ = +32.1° (MeOH, 1.18%, 20 °C). ¹H NMR (400 MHz, CDCl₃) δ_H (ppm) 7.93 (d, *J* = 8.12 Hz, 2H), 7.26–7.47 (m, 7H), 7.19 (t, *J* = 7.34 Hz, 1H), 7.05 (d, *J* = 8.12 Hz, 2H), 6.70 (s, 1H), 5.08 (s, 1H), 2.94–3.59 (m, 6H). ¹³C NMR (100 MHz, CDCl₃) δ_C (ppm) 171.2, 149.8, 144.1, 143.8, 143.0, 142.7, 141.0, 130.4, 2 × 129.8, 2 × 129.4, 128.5, 126.9, 126.7, 126.0, 124.7, 124.5, 124.1, 123.2, 120.3, 81.6, 55.9, 43.1, 39.9, 37.9. HRMS (ESI) *m/z* calculated for C₂₆H₂₂O₃ (M − H)⁺, 381.1485; found, 381.1488.

N-Methyl-D-glucamide Salt of 4-(((1S,2S)-2,3-Dihydro-1-hydroxy-2-(1H-inden-2-yl)-1H-inden-2-yl)methyl)benzoic Acid (1). To the MeOH (HPLC grade, 10 mL) suspension of the acid **16** (1.08 g, 2.8 mmol) at 55 °C was added N-methyl-D-glucamine (0.55 g, 2.8 mmol, 1 equiv) portionwise. This mixture was stirred at 55 °C until a clear solution was obtained. The solution was then hot-filtered into a clean flask and allowed to cool. Isopropyl alcohol (20 mL) was then added to precipitate the salt. The salt was then filtered and washed with acetonitrile (20 mL), sucked dry, and then dried in a vacuum oven at 40 °C. The title salt (1.61 g, 98%) was obtained as a white solid; mp 165–167 °C. Optical rotation: [α]_D²⁰ = −88.6° (MeOH, 70 mg/10 mL, 20 °C). ¹H NMR (400 MHz, DMSO-*d*₆) δ_H (ppm) 7.62 (d, *J* = 7.96 Hz, 2H), 7.39–7.33 (m, 2H), 7.25–7.18 (m, 4H), 7.15 (t, *J* = 7.34 Hz, 1H), 7.06 (t, *J* = 7.26 Hz, 1H), 6.81 (d, *J* = 8.04 Hz, 2H), 6.39 (s, 1H), 5.81 (broad s, 1H), 5.03 (s, 1H), 3.84–3.80 (m, 1H), 3.64 (broad d, *J* = 4.92 Hz, 1H), 3.59–3.35 (m, 6H), 3.14 (d, *J* = 13.56 Hz, 1H), 3.00–2.76 (m, 4H), 2.64 (d, *J* = 13.60 Hz, 1H), 2.42 (apparent s, 3H). ¹³C NMR (150 MHz, DMSO-*d*₆) δ_C (ppm) 169.5, 154.2, 145.1, 144.4, 142.8, 141.7, 140.3, 133.6, 2 × 129.2, 2 × 128.5, 127.5, 127.0, 126.2, 126.0, 124.4, 124.2, 123.7, 123.4, 120.1, 81.0, 71.2, 70.5, 70.3, 69.3, 63.5, 55.7, 51.8, 39.4, 38.2, 37.9, 33.9. HRMS (ESI) *m/z* calculated for C₃₃H₃₉O₈N (M − H)⁺, 576.2592; found, 576.2612.

N-Methyl-D-glucamine Salt of 4-(((1S,2R)-2,3-Dihydro-1-hydroxy-2-(1H-inden-2-yl)-1H-inden-2-yl)methyl)benzoic Acid (20). To the MeOH (HPLC grade, 1 mL) solution of the acid **19** (0.2 g, 0.52 mmol, 1 equiv) at 55 °C was added a MeOH (2 mL) suspension of N-methyl-D-glucamine (0.102 g, 0.52 mol, 1 equiv). This mixture was stirred at room temperature overnight. Since no filterable material was obtained, the solvent was evaporated completely under reduced pressure and the resulting solid was slurried in EtOAc. The salt was filtered, washed with EtOAc, and then dried in vacuum oven at 40 °C. The title salt (0.222 g, 74%) was obtained as a pale-yellow solid; mp 70–80 °C (decomp/hygroscopic). Optical rotation: [α]_D²⁰ = +63.3° (MeOH, 32 mg/10 mL, 20 °C). ¹H NMR (400 MHz, DMSO-*d*₆) δ_H (ppm): 7.69 (t, *J* = 7.92 Hz, 2H), 7.37 (d, *J* = 7.32 Hz, 1H), 7.33–7.20 (m, 5H), 7.15 (t, *J* = 7.46 Hz, 1H), 7.06 (t, *J* = 7.28 Hz, 1H), 6.91 (d, *J* = 8.00 Hz, 2H), 6.38 (s, 1H), 5.45 (broad s, 1H), 4.97 (s, 1H), 3.89–3.87 (m, 1H), 3.67 (broad d, *J* = 4.80 Hz, 1H), 3.61–3.38 (m, 6H), 3.17 (t, *J* = 14.84 Hz, 1H), 2.98–2.80 (m, 4H), 2.47 (apparent s, 3H). ¹³C NMR (100 MHz, DMSO-*d*₆) δ_C (ppm) 170.2, 152.7, 144.9, 144.7, 143.5, 141.4, 140.6, 135.1, 2 × 129.3, 2 × 128.6, 128.3, 127.7, 126.3, 125.9, 124.5, 124.4, 123.5, 123.3, 120.0, 80.9, 71.3, 70.5, 70.3, 68.9, 63.5, 55.9,

51.5, 42.4, 39.6, 38.2, 33.4. HRMS (ESI) m/z calculated for $C_{33}H_{39}O_8N$ ($M - H$)⁺, 576.2592; found, 576.2616.

Biological Assays. Animals and Experimental Design. Specific Pathogen-Free female BALB/c strain mice, 6–8 weeks of age, were obtained from a commercial supplier (Harlan, UK). Mice were fed irradiated diet and housed in individually ventilated cages (Tecniplast, UK) under positive pressure. IL-10^{-/-} mice, on a BALB/c strain background, were initially purchased from Jackson Laboratories (USA) and then bred under specific pathogen-free (SPF) conditions at Trinity College Dublin. In mouse studies, experimental groups were randomly alphabetically labeled. Throughout experiments, all data recording and analysis was performed in a blind manner.

All animal experiments were performed in compliance with Irish Department of Health and Children regulations and were approved by the Trinity College BioResources ethical review board.

Compounds. DSS (35–50000 kDa) was purchased from (ICN Biomedical Inc., USA). Prednisolone was obtained from Sigma Aldrich. All compounds were prepared for oral gavage (0.1 mL po per 10 g body weight) as an aqueous solution in distilled water. Distilled water was used as a vehicle control.

Dextran Sulfate Sodium (DSS) Model. A 5% DSS solution was prepared in drinking (tap) water, with fresh DSS solution provided every second day. The mice were checked each day for morbidity and the weight of individual mice recorded. Induction of colitis was determined by weight loss, fecal blood, stool consistency, and, upon autopsy, length of colon and histology. Approximately 1 cm of distal colon was removed for histology. The rest of the colon was recovered, snap-frozen, and stored at -20°C for immunological analysis. To quantify the severity of colitis, a disease activity index (DAI) was determined based on previous studies of DSS-induced colitis.⁶ DAI was calculated for individual mice on each day based on weight loss, occult blood, and stool consistency. A score was given for each parameter, with the sum of the scores used as the DAI (Weight loss 0% > 9%: 0–4. Stool consistency: 0, 2, 4 as normal, loose stool, and diarrhea. Stool blood: 0, 2, 4 as none, visible, and gross bleeding. Maximum score is 12).

Sections of distal colon were fixed in 10% formaldehyde–saline. Tissue was paraffin-embedded and 5 μm serial sections cut. Slides were stained with hematoxylin and eosin. Histological grading was based on a scoring system (Severity of cell infiltration: 0–3 for none, slight, moderate, and severe. Extent of injury: 0–3 for none, mucosal, mucosal and submucosal, transmural. Crypt damage: 0–4 for none, basal 1/3 damaged, basal 2/3 damaged, only surface epithelium intact, loss of entire crypt, and epithelium.) modified from previous studies on DSS-induced colitis and histology scoring was performed in a blinded fashion independently by two observers. The combined score from each feature graded was calculated for individual mice with the maximum score being 10. After removal of approximately 1 cm of colon for histology, the remainder of the colon was snap-frozen and stored. Individual colon tissue samples were thawed, and gut contents were removed, chopped finely, and homogenized. The protein concentration of the supernatant was determined. Colon levels of myeloperoxidase (MPO) were determined using a standard method.³⁵ Cytokines in colon supernatants were analyzed using conventional sandwich ELISAs.³⁵ Coating antibodies, standards, and detecting antibodies were obtained from BDPharMingen or R&D Systems. Levels of cytokines and MPO are expressed relative to colon protein.

Power calculations on data from previous studies have shown that a sample of size of at least six will detect significant difference ($P < 0.05$) between groups using the acute 5% DSS model. In these studies, eight mice were used in each group. Statistical differences between multiple groups were determined by ANOVA and Dunnett multiple comparison test as a post-test.

IL-10^{-/-} Colitis Model. Female 6–8 week old IL-10-mice were randomized into two groups of 12 mice. Mice were checked weekly for rectal prolapse and/or bleeding, and mice with overt colitis were killed. Compound 1 was prepared for oral gavage (0.1 mL po per 10 g body weight) weekly from individual tubes of dry powder by dissolving the compound in the required volume of distilled water as vehicle. Animals were dosed with 1 (300 mg/kg/week) or vehicle, according to a Mon/Wed/Fri dosing schedule, for nine weeks. Experimental groups were

randomly alphabetically labeled. When mice were killed, a 1 cm piece of the proximal colon was removed from IL-10-mice. All tissues were fixed in 10% formaldehyde–saline, and sections were prepared and stained with hematoxylin and eosin, as described.³⁶ All histology scoring was performed in a blinded fashion independently by two observers. Colon sections from mice were graded using a histological index ranging from 0 to 4, based on the degree of epithelial layer erosion, goblet cell depletion, and inflammatory cell infiltrate³⁷ (0 = normal, 1 = minimal evidence of inflammatory infiltrate, 2 = significant evidence of inflammatory infiltrate (cryptitis, crypt abscesses), 3 = significant evidence of inflammatory infiltrate with goblet cell depletion, 4 = significant evidence of inflammatory infiltrate with erosion of the mucosa). The maximum possible score was 4. Serum amyloid A (SAA) was measured by sandwich ELISA using a kit from Life Diagnostics Inc. (PA, USA). SAA ELISAs were performed following the manufacturer's instructions. All data are means and SEM from 11 1-treated mice and nine vehicle mice, and statistical analysis was made by Student's t test.

■ AUTHOR INFORMATION

Corresponding Author

*For N.H.F.: phone, +353-1-8962825; fax, 353-1-89628210; E-mail, nfrnkish@tcd.ie. For H.S.: phone, +353-1-8962828; fax, 353-1-89628210; E-mail, hsheridn@tcd.ie.

Author Contributions

The authors contributed equally to this work.

Notes

The authors declare the following competing financial interest(s): N Frankish and H Sheridan are co-founders of Trino Therapeutics Ltd.

■ ACKNOWLEDGMENTS

This work was supported by The Wellcome Trust, grant reference no. 067033/Z/02/A, Enterprise Ireland, and Trino Therapeutics Ltd.

■ ABBREVIATIONS USED

Aq, aqueous; DCM, dichloromethane; EtOAc, ethyl acetate; NH_4Cl , ammonium chloride; MgSO_4 , magnesium sulfate; MeOH, methanol; NaBH_4 , sodium borohydride; Rt, retention time; CD, Crohn's disease; DSS, dextran sulfate sodium; DAI, disease activity index; IBD, inflammatory bowel diseases; IFN γ , interferon gamma; IL-10, interleukin-10; LPS, lipopolysaccharide; MPO, myeloperoxidase; NF- κB , nuclear factor-kappaB; NRs, nuclear receptors; SAA, serum amyloid A; UC, ulcerative colitis; SPF, specific pathogen-free; MPO, myeloperoxidase

■ REFERENCES

- (1) Talley, N. J.; Abreu, M. T.; Achkar, J. P.; Bernstein, C. N.; Dubinsky, M. C.; Hanauer, S. B.; Kane, S. V.; Sandborn, W. J.; Ullman, T. A.; Moayyedi, P. An evidence-based systematic review on medical therapies for inflammatory bowel disease. *Am. J. Gastroenterol.* **2011**, *106* (Suppl 1), S2–25 quiz S26.
- (2) Maloy, K. J.; Powrie, F. Intestinal homeostasis and its breakdown in inflammatory bowel disease. *Nature* **2011**, *474*, 298–306.
- (3) Mowat, C.; Cole, A.; Windsor, A.; Ahmad, T.; Arnott, L.; Driscoll, R.; Mitton, S.; Orchard, T.; Rutter, M.; Younge, L.; Lees, C.; Ho, G. T.; Satsangi, J.; Bloom, S. Guidelines for the management of inflammatory bowel disease in adults. *Gut* **2011**, *60*, 571–607.
- (4) Bosani, M.; Ardizzone, S.; Porro, G. B. Biologic targeting in the treatment of inflammatory bowel diseases. *Biologics* **2009**, *3*, 77–97.
- (5) Melmed, G. Y.; Targan, S. R. Future biologic targets for IBD: potentials and pitfalls. *Nature Rev. Gastroenterol. Hepatol.* **2010**, *7*, 110–117.

- (6) Cooper, H. S.; Murthy, S. N.; Shah, R. S.; Sedergran, D. J. Clinicopathologic study of dextran sulfate sodium experimental murine colitis. *Lab. Invest.* **1993**, *69*, 238–249.
- (7) Berg, D. J.; Davidson, N.; Kuhn, R.; Muller, W.; Menon, S.; Holland, G.; Thompson-Snipes, L.; Leach, M. W.; Rennick, D. Enterocolitis and colon cancer in interleukin-10-deficient mice are associated with aberrant cytokine production and CD4(+) TH1-like responses. *J. Clin. Invest.* **1996**, *98*, 1010–1020.
- (8) Donnelly, D. M. X.; O'Reilly, J.; Polonsky, J.; Sheridan, M. H. Biosynthesis of Fomajorin-D-Incorporations of [1-C-13]-, [2-C-13]-, and [1,2-C-132]-Acetates. *J. Chem. Soc., Chem. Commun.* **1983**, 615–616.
- (9) Donnelly, D. M. X.; O'Reilly, J.; Polonsky, J.; Sheridan, M. H. In Vitro Production and Biosynthesis of Fomajorin-D and Fomajorin-S by Fomes-Annosus (Fr) Cooke. *J. Chem. Soc., Perkin Trans. 1* **1987**, 1869–1872.
- (10) Jaki, B.; Orjala, J.; Burgi, H. R.; Sticher, O. Biological screening of cyanobacteria for antimicrobial and molluscicidal activity, brine shrimp lethality, and cytotoxicity. *Pharm. Biol.* **1999**, *37*, 138–143.
- (11) Chen, Y. H.; Chang, F. R.; Lu, M. C.; Hsieh, P. W.; Wu, M. J.; Du, Y. C.; Wu, Y. C. New benzoyl glucosides and cytotoxic pteroin sesquiterpenes from *Pteris ensiformis* burm. *Molecules* **2008**, *13*, 255–266.
- (12) Syrchina, A. I.; Semenov, A. A. Natural Indanones. *Khim. Prir. Soedin.* **1982**, 3–14.
- (13) Okpekon, T.; Millot, M.; Champy, P.; Gleye, C.; Yolou, S.; Bories, C.; Loiseau, P.; Laurens, A.; Hocquemiller, R. A novel 1-indanone isolated from *Uvaria afzelii* roots. *Nat. Prod. Res.* **2009**, *23*, 909–915.
- (14) Ito, T.; Tanaka, T.; Inuma, M.; Nakaya, K.; Takahashi, Y.; Sawa, R.; Murata, J.; Darnaedi, D. Three new resveratrol oligomers from the stem bark of *Vatica pauciflora*. *J. Nat. Prod.* **2004**, *67*, 932–937.
- (15) Vacca, J. P.; Dorsey, B. D.; Schleif, W. A.; Levin, R. B.; McDaniel, S. L.; Darke, P. L.; Zugar, J.; Quintero, J. C.; Blahy, O. M.; Roth, E.; Sardana, V. V.; Schlabach, A. J.; Graham, P. I.; Condra, J. H.; Gotlib, L.; Holloway, M. K.; Lin, J.; Chen, I. W.; Vastag, K.; Ostovic, D.; Anderson, P. S.; Emini, E. A.; Huff, J. R. L-735,524—An Orally Bioavailable Human-Immunodeficiency-Virus Type-1 Protease Inhibitor. *Proc. Natl. Acad. Sci. U.S.A.* **1994**, *91*, 4096–4100.
- (16) Lin, J. H. Role of pharmacokinetics in the discovery and development of indinavir. *Adv. Drug. Delivery Rev.* **1999**, *39*, 33–49.
- (17) Jelic, V.; Darreh-Shori, T. Donepezil: A Review of Pharmacological Characteristics and Role in the Management of Alzheimer Disease. *Clin. Med. Ins. Ther.* **2010**, *2*, 771.
- (18) Oldfield, V.; Keating, G. M.; Perry, C. M. Rasagiline: a review of its use in the management of Parkinson's disease. *Drugs* **2007**, *67*, 1725–1747.
- (19) Schepers, M. A.; Nikitakis, N. G.; Chaisuparat, R.; Montaner, S.; Sauk, J. J. Sulindac induces apoptosis and inhibits tumor growth in vivo in head and neck squamous cell carcinoma. *Neoplasia* **2007**, *9*, 192–199.
- (20) Shiff, S. J.; Qiao, L.; Tsai, L. L.; Rigas, B. Sulindac sulfide, an aspirin-like compound, inhibits proliferation, causes cell cycle quiescence, and induces apoptosis in HT-29 colon adenocarcinoma cells. *J. Clin. Invest.* **1995**, *96*, 491–503.
- (21) Ho, S.-T.; Yang, M.-S.; Wu, T.-S.; Wang, C.-H. Studies on the Taiwan Folk Medicine: III. A Smooth Muscle Relaxant from *Onychium siliculosum*, Onitin. *Planta Med.* **1985**, 148–150.
- (22) Yang, M. S. Studies on the Taiwan folk medicine. VI. Studies on onitin. *Planta Med.* **1986**, 25–27.
- (23) Sheridan, H.; Lemon, S.; Frankish, N.; McArdle, P.; Higgins, T.; James, J. P.; Bhandari, P. Synthesis and antispasmodic activity of nature identical substituted indanes and analogs. *Eur. J. Med. Chem.* **1990**, *25*, 603–608.
- (24) Sheridan, H.; Frankish, N.; Farrell, R. Smooth muscle relaxant activity of pteroin Z and related compounds. *Planta Med.* **1999**, *65*, 271–272.
- (25) Sheridan, H.; Frankish, N.; Farrell, R. Synthesis and antispasmodic activity of analogues of natural pteroin Z. *Eur. J. Med. Chem.* **1999**, *34*, 953–966.
- (26) Farrell, R.; Kelleher, F.; Sheridan, H. Synthesis of fern sesquiterpene pteroin Z via a novel palladium-catalyzed route. *J. Nat. Prod.* **1996**, *59*, 446–447.
- (27) Frankish, N.; Farrell, R.; Sheridan, H. Investigation into the mast cell stabilizing activity of nature-identical and synthetic indanones. *J. Pharm. Pharmacol.* **2004**, *56*, 1423–1427.
- (28) Sheridan, H.; Walsh, J. J.; Cogan, C.; Jordan, M.; McCabe, T.; Passante, E.; Frankish, N. H. Diastereoisomers of 2-benzyl-2,3-dihydro-2-(1H-inden-2-yl)-1H-inden-1-ol: potential anti-inflammatory agents. *Bioorg. Med. Chem. Lett.* **2009**, *19*, 5927–5930.
- (29) Sheridan, H.; Walsh, J. J.; Jordan, M.; Cogan, C.; Frankish, N. A series of 1,2-coupled Indane dimers with mast cell stabilisation and smooth muscle relaxation properties. *Eur. J. Med. Chem.* **2009**, *44*, 5018–5022.
- (30) Frankish, N.; Sheridan, H. Unpublished results on Stereochemistry, 2012.
- (31) Frankish, N.; Sheridan, H. Unpublished Solubility and Pharmacokinetic Studies, 2012.
- (32) Ford, A. C.; Achkar, J. P.; Khan, K. J.; Kane, S. V.; Talley, N. J.; Marshall, J. K.; Moayyedi, P. Efficacy of 5-aminosalicylates in ulcerative colitis: systematic review and meta-analysis. *Am. J. Gastroenterol.* **2011**, *106*, 601–616.
- (33) Benchimol, E. L.; Seow, C. H.; Otley, A. R.; Steinhart, A. H. Budesonide for maintenance of remission in Crohn's disease. *Cochrane DB Syst. Rev.* **2009**, CD002913.
- (34) Frankish, N.; Sheridan, H. Unpublished Toxicology Observations, 2012.
- (35) Cummins, E. P.; Seeballuck, F.; Keely, S. J.; Mangan, N. E.; Callanan, J. J.; Fallon, P. G.; Taylor, C. T. The hydroxylase inhibitor dimethylallylglycine is protective in a murine model of colitis. *Gastroenterology* **2008**, *134*, 156–165.
- (36) Axelsson, L. G.; Landstrom, E.; Bylund-Fellenius, A. C. Experimental colitis induced by dextran sulphate sodium in mice: beneficial effects of sulphasalazine and olsalazine. *Aliment. Pharmacol. Ther.* **1998**, *12*, 925–934.
- (37) L'Heureux, M. C.; Brubaker, P. L. Glucagon-like peptide-2 and common therapeutics in a murine model of ulcerative colitis. *J. Pharmacol. Exp. Ther.* **2003**, *306*, 347–354.